ENVIRONMENTAL SCIENCE ARCHIVES
ISSN: 2583-5092
Volume V Issue 1, 2026
www.envsciarch.com

RESEARCH PAPER OPEN ACCESS

Valorizing Kitchen Waste into Potent Nano-Remediators: A Green Synthesis of Iron Oxide Nanoparticles using *Punica granatum* for Efficient Industrial Dye Decolouration

Received:
2025/12/20
Accepted:
2026/01/16
Published:
2026/01/20

Neha Gaur and Anuya Verma
Department of Environmental Sciences, Vigyan Bhawan, Block-B, New Campus, M.L. Sukhadia University, Udaipur, Rajasthan, India
*Correspondence for materials should be addressed to NG (email: nehagour230059@gmail.com)

Abstract
In the quest for sustainable nanomaterials and eco-friendly wastewater treatment technologies, this study presents a green synthesis of iron oxide (Fe_2O_3) nanoparticles utilizing commonly discarded kitchen waste—pomegranate peels (*Punica granatum*). The synthesized nanoparticles were extensively characterized using UV-Vis spectroscopy, XRD, FTIR, SEM and TEM, confirming the presence of crystalline α-Fe_2O_3 phase by pomegranate peel while no distinctive peak suggesting amorphous nature of Fe_2O_3. Their catalytic performance was assessed in the decolouration of six industrially significant dyes- Methylene blue, Acid orange 7, Basic Dyes Malachite, Direct red 12B, Disperse yellow 3 and Reactive Black 5. *Punica granatum* mediated Fe_2O_3 nanoparticles showed significant dye removal efficiency. Notably, ~90% decolouration of all the dyes was achieved within 90 minutes by derived Fe_2O_3. The analysis highlighted that *Punica granatum* peel extract is the superior biogenic source, making the resulting Fe_2O_3 NPs highly effective candidates for treating diverse industrial dyes in polluted water streams. The study contributes to circular economy strategies and promotes green chemistry in nanotechnology and environmental remediation.

Keywords: Kitchen waste; Pomegranate peel; Iron oxide nanoparticles; Dye decolouration

Introduction

Iron nanoparticles are highly reactive, cost-efficient, easy to make, have a varied range of applications, and are less toxic than TiO_2, ZnO and Ag NPs. The versatility of iron nanoparticles extends to their ability to be functionalized with various coatings, which enhances their stability and targeting capabilities (Siciliano et al., 2022; Thacker et al., 2019). These nanoparticles have shown promising results in environmental remediation, particularly in the treatment of contaminated water and soils. Furthermore, iron nanoparticles have gained attention in the medical field for their potential use in targeted drug delivery and as contrast agents in magnetic resonance imaging (Jahangirian et al., 2019). Iron nanoparticles are used in various sectors, such as medicine, optics, electronics, sensing and environmental remediation, owing to their strong adsorption and redox potential (Abdulwahid et al., 2022; Wang et al., 2020).

Various forms of iron nanoparticles, such as maghemite (γ-Fe_2O_3), hematite (α- Fe_2O_3), magnetite (Fe_3O_4) and metallic zerovalent iron, were produced. Several studies have indicated that a reduction in the size of iron particles results in an increased surface area, which is directly proportional to an enhanced reaction rate and the availability of free iron atoms.

Several methodologies for synthesizing iron oxide nanoparticles include thermal decomposition, co-precipitation, sol-gel and microemulsion techniques (Dadfar et al., 2019). Each of these methods has distinct advantages and disadvantages, with most being chemically based, potentially releasing harmful chemicals into the environment. Conversely, green synthesis offers a renewable approach that can be effectively integrated with chemical methods to produce the desired nanoparticles, as it is readily accessible, cost-effective and sustainable (Siwal et al., 2021). Kitchen waste (KW), also known as organic or food waste, can have detrimental effects on the environment if improperly managed. Several studies have demonstrated the use of plantain peel extract (Venkateswarlu et al., 2013), banana peel extract (Majumder et al., 2019), orange peel (Skiba and Vorobyova, 2019), eggshells (Habte et al., 2019), papaya peel extract (Phang Y-K et al., 2021), Carica papaya leaf extracts (Rathnasamy et al., 2017), grape waste (Krishnaswamy et al., 2014), *Tamarindus indica* (Tamarind) fruit shell (Gomathi et al., 2020), Sapota fruit waste (Vishwasrao et al., 2019), pomegranate peel extract (Patel et al., 2019) and onion peel extract (Patra et al., 2016) for the preparation of nanoparticles.

The peel of *Punica granatum*, is a significant byproduct of agriculture, making up 40-50% of the fruit's overall mass. Instead of being a waste issue, this peel is a rich source of bioactive substances, especially ellagitannins (such as punicalagin) and gallotannins. These polyphenolic compounds are characterized by numerous hydroxyl (OH) and carbonyl (C=O) functional groups, which render the aqueous extract of pomegranate peel (PPE) an exceptionally efficient, easily accessible and cost-effective natural material for the eco-friendly synthesis of nanomaterials. The use of this agricultural waste fits seamlessly with the principles of a circular economy and sustainable resource management.

This study highlighted the utilization of pomegranate peel *(Punica granatum)* plant extracts to produce iron oxide nanoparticles (Fe_2O_3 NPs). The study evaluates the photocatalytic performance of green-synthesized Fe_2O_3 for the swift and thorough decolorization of various dyes, including Methylene blue, Acid orange 7, Basic Dyes Malachite, Direct red 12B, Disperse yellow 3 and Reactive Black 5 under exposure of sunlight.

Materials and methods

Collection and processing of pomegranate and red peanut peels

Pomegranate peels were sourced from a nearby market. After being thoroughly rinsed with double distilled water, they were air-dried in a shaded area, away from direct sunlight. Once dried, the peels were ground using an electric grinder and then sieved to obtain particles sized between 60 and 40 mesh. Ten grams of these particles were mixed with 500 ml of distilled water in a beaker and heated to 80°C for 15 minutes. After cooling to room temperature, the extract was filtered through 0.45 µm filter paper. The resulting light-yellow solution was immediately used for reactions with the Fe^{3+} solution.

Synthesis of iron oxide nanoparticles

PPE (Pomegranate Peel Extract) was used to synthesize Fe_2O_3 nanoparticles (NPs). A 0.01 M solution of Fe^{3+} was combined with PPE at 20 g/l and stirred at room temperature for 5 minutes without additional agents. After three days, a black precipitate of Fe_2O_3 NPs formed. The mixture was heated to reduce volume by half, centrifuged at 11,000 rpm for 10 minutes, and the nano-powder was washed with ethanol and vacuum-dried.

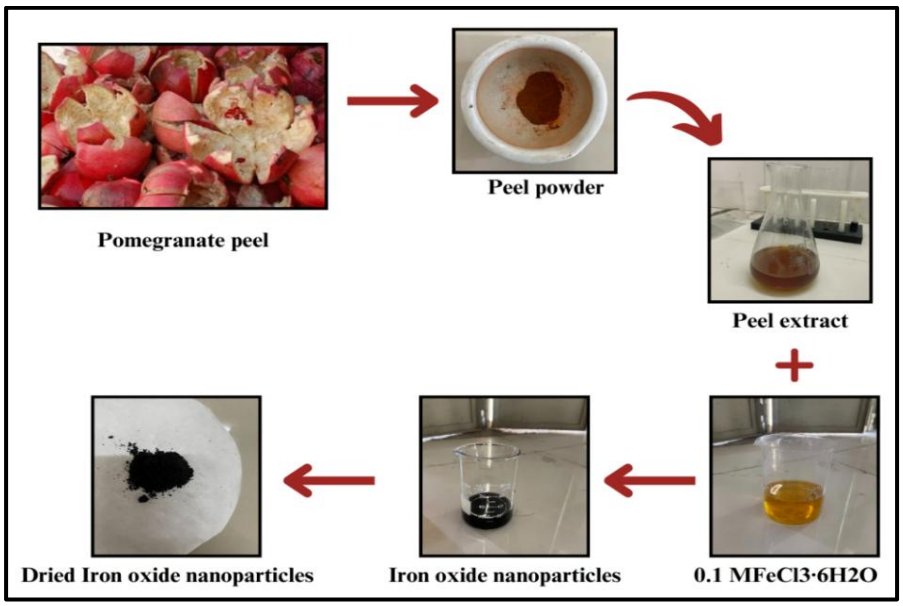

Fig. 1. Schematic representation of Fe_2O_3 NPs synthesized using Pomegranate peel extract

Characterization of synthesized Fe_2O_3 nanoparticles

The synthesized Fe_2O_3 nanoparticles were subjected to a comprehensive analysis of their physicochemical properties to assess their structural, morphological and functional characteristics. The characterization of the Fe_2O_3 nanoparticles was conducted using several techniques. X-ray Diffraction (XRD) analysis was performed utilizing a Panalytical X'pert Pro X-ray diffractometer, operating within the 2θ range of 5° to 40°, with a step size of 0.02° and a scanning rate of 1° per minute. The analysis employed Cu-Kα radiation (λ = 1.54 Å) at a voltage of 50 kV and a current of 40 mA.

Surface characteristics were examined using a JEOL (Japan) JSM 6100 scanning electron microscope. Dye concentrations in aqueous solutions were measured using a UV-visible spectrophotometer (JASCO V-750) both before and after adsorption. Fourier-transform infrared (FTIR) analysis was conducted using a Perkin Elmer Spectrum GX, covering a wavenumber range from 500 cm^{-1} to 4000 cm^{-1}, to verify the presence of functional groups in the adsorbents.

Dye decolorization experiments

To investigate the photocatalytic properties of the synthesized nanoparticles, various solutions of Methylene blue, Acid orange 7, Basic Dyes Malachite, Direct red 12, Disperse yellow 3 and Reactive Black 5 were prepared at concentrations of 20 mg/L, 40 mg/L, 60 mg/L, 80 mg/L, and 100 mg/L. A 50 ml sample of each dye solution was placed in a beaker with different amounts of synthesized nanoparticles (0.2 g/L, 0.4 g/L, 0.6 g/L, 0.8 g/L, and 1.0 g/L) and exposed to sunlight while being continuously stirred. Samples of the dye solution were taken at intervals of 5, 10, 20, 30, 60, 120, and 180 minutes to assess changes in dye concentration.
The effectiveness of iron particles in decolorizing the dye was evaluated using

$$\textbf{Dye Decoloration Efficiency}\ (\%) = \left(\frac{Co - Ct}{Co}\right) \times 100$$

where Co and Ct represent the dye concentrations at the start and after a reaction time of t (minutes), respectively. The interaction between dye molecules and iron particles was examined by altering the iron dosage (0.2–1 g/L) and dye concentration (20–100 mg/L).

Results and discussions

Characteristics of PPE Fe_2O_3NPs

The synthesis of Fe_2O_3 nanoparticles (NPs) led to noticeable color transformations in the extract mixture. Initially, the solution's red hue shifted to black upon reacting with ferric chloride hexahydrate, and it turned green after the Fe_2O_3 NPs were removed through filtration.

The SEM micrographs of α-Fe_2O_3 nanoparticles synthesized using pomegranate peel extract reveal a well-aggregated spherical shape. In UV-visible spectroscopy, an absorption peak indicates that electrons are taking in energy within the 200-800 nm wavelength range. The absorption spectrum for iron oxide nanoparticles, when excited at 274 nm, corresponds to Fe_2O_3 NPs. A significant absorption peak observed in PPE-synthesized Fe_2O_3 NPs between 270–320 nm suggests Fe-O charge transfer, confirming the presence of iron oxide nanoparticles.

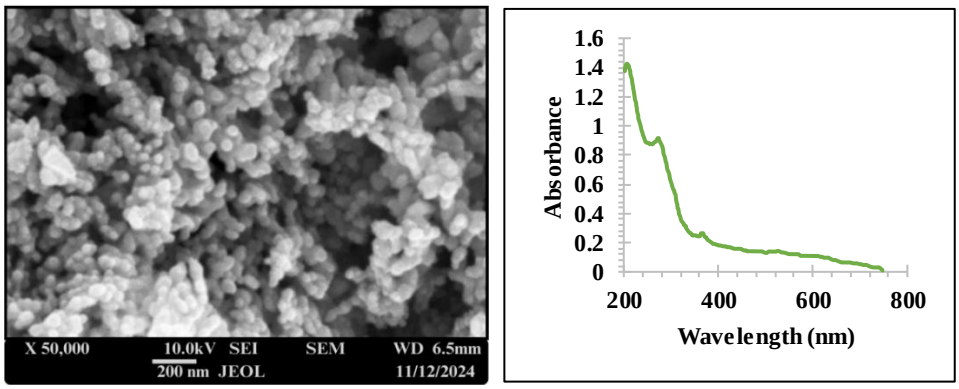

Fig. 2. SEM image and UV-Vis spectra of Fe_2O_3 NPs using the extract of Pomegranate peel

FTIR analysis offers insights into the alteration of certain surface functional groups that may have been involved in the chemical modification process. Figure 3 (a) illustrates the FTIR spectra of Pomegranate peel extract (PPE) and the synthesized MNPs. A broad peak at 3503 cm^{-1} is observed, which is attributed to the O-H stretching vibration of phenolic compounds. Meanwhile, the peaks at 2926 cm^{-1} are likely due to the C–H stretching of methyl groups, with stretching vibrations of -CH_3 or -CH_2 groups in carboxylic acid. The peak around 1711 cm^{-1} is associated with

C=O stretching vibration. Peaks at 1376 and 1267 cm^{-1} may correspond to C-O acid stretching groups. The emergence of two entirely new peaks at approximately 627 and 553 cm^{-1} in Fe_2O_3 NPs is linked to the Fe-O stretching band, providing strong evidence of chemical interactions between Fe and oxygen (Fe O) vibration.

Figure 3 (b) illustrates the XRD pattern of Fe_2O_3 nanoparticles synthesized using pomegranate peel extract. The diffraction peaks were observed at 2θ values approximately 24.303, 31.806, 33.314, 35.795, 41.048, 45.604, 49.616, 54.240, 57.759, 62.570, and 64.134, which correspond to the (012), (220), (104), (110), (113), (400), (024), (116), (018), (214) and (300) planes of crystalline Fe_2O_3 NPs, respectively. These peaks align with the hematite phase of iron oxide (α-Fe2O3), indicating a rhombohedral crystal structure. The EDS analysis of the iron oxide nanoparticles from PPE-iron oxide nanoparticles indicated that the composition of Fe and oxygen was 70.08% and 20.04%, respectively. The most prominent energy peaks were observed at approximately 0.25 and 6.8 keV.

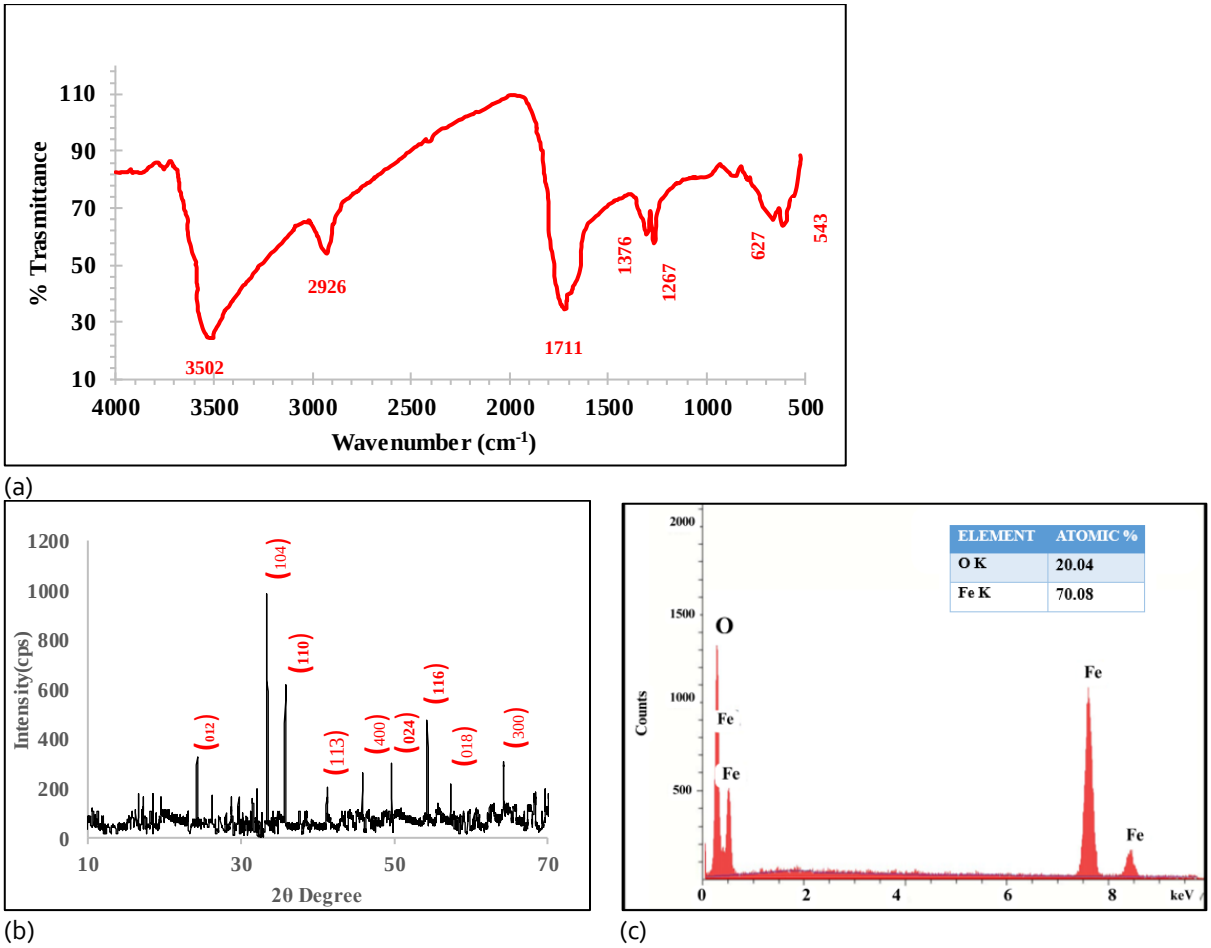

Fig. 3. (a) FTIR, (b) XRD and (c) EDS graph of Fe_2O_3 NPs using the extract of Pomegranate peel

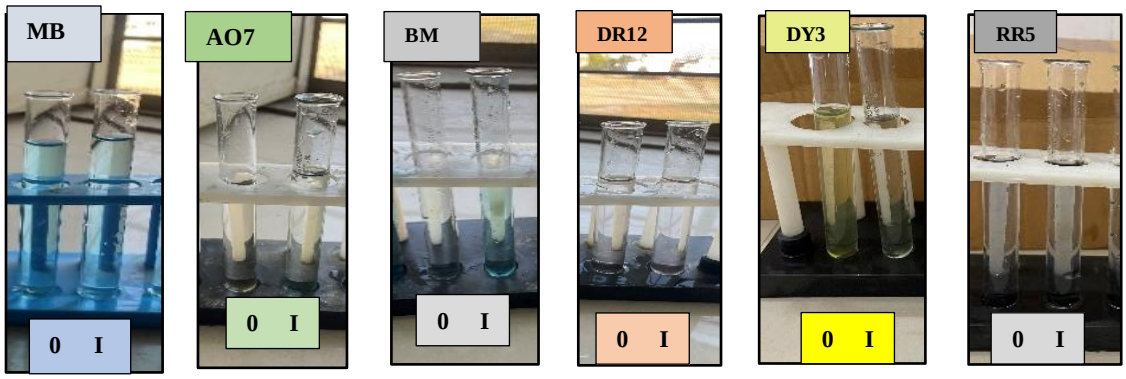

Fig. 4. Effect of initial concentration of dyes on decolouration efficiency. O- initial concentration 20 mg/L, I- Pomegranate peel mediated Fe_2O_3NPs

Dye decolorization efficiency

Initial dye concentration

Figure 4 illustrates how the initial concentration of dyes affects the removal percentage of MB, AO7, BM, DR12, DY3 and RB5 dyes. The figure clearly shows that the removal efficiency for all dyes is at its peak when the

concentration is at its lowest (20 mg/L), with removal percentages ranging from 80% to 100%. This suggests that the synthesized iron oxide nanoparticles exhibit a strong initial capability to degrade dyes at lower concentrations. This enhanced removal can be attributed to the greater availability of binding sites at these lower concentrations, leading to a higher percentage of MB, AO7, BM, DR12, DY3 and RB5 dyes being removed. (Badeenezhad et al., 2019; Bhuiyan et al., 2020)As depicted in Figure 5, iron oxide nanoparticles derived from *Punica granatum* L. (Pomegranate) Peel demonstrate that Methylene Blue achieves the highest removal rate at lower concentrations, reaching up to 98.63% at 20 mg/L. In contrast, Direct Red 12 shows the least removal efficiency at 100 mg/L, with a rate of 62%. Generally, as the dye concentration increases, the removal efficiency tends to decrease, likely due to the saturation of the nanoparticles active sites. This pattern is consistent across all dyes, with degradation percentages ranging from 62% to 76% at the maximum concentration of 100 mg/L.

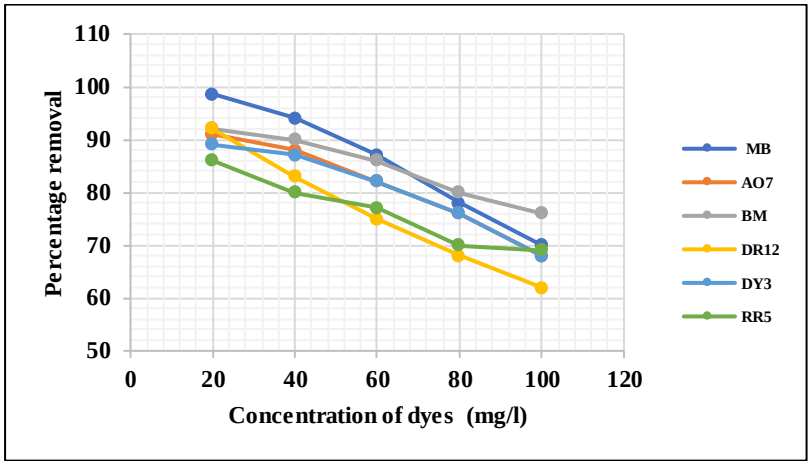

Fig. 5. Graphs showing the effect of the initial concentration of dyes on the percentage removal of dyes using Pomegranate peel mediated Fe_2O_3NPs

Iron oxide nanoparticle dose (adsorbent dose)

The findings indicated a connection between the dye removal percentage and the amount of adsorbent used. It was observed that increasing the dosage of iron oxide nanoparticles from 0.2 g to 1.0 g enhances the reactive sites of iron, leading to maximum dye decolorization (Badeenezhad et al., 2019; Nassar et al., 2015).

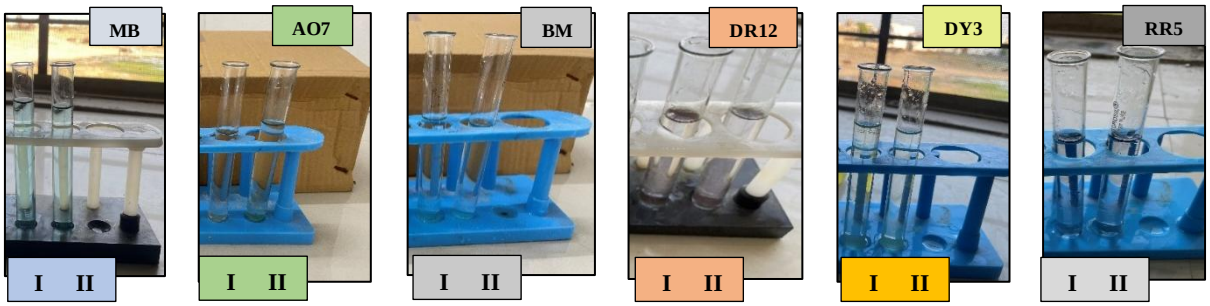

Fig. 6. Effect of 0.8 g/L adsorbent dose on the decolouration of dyes by Pomegranate peel mediated Fe_2O_3NPs

The use of *Punica granatum L.* (Pomegranate) peel to mediate Fe_2O_3 NPs significantly boosts dye removal efficiency for all tested dyes, with the best results achieved at a concentration of 0.8 g/L. At this level, MB shows the highest removal rate of 98%, while BM and AO7 also achieve impressive efficiencies of 92.78% and 95.12%, respectively. Increasing the adsorbent dose beyond this point leads to a plateau or slight decline in removal efficiency, indicating that saturation occurs around 0.8 g/L, where adsorption sites are fully occupied, and further increases yield diminishing returns.

Contact time is a crucial factor in examining dye degradation, especially in the context of heterogeneous photocatalysis with materials such Pomegranate peel mediated Fe_2O_3 NPs. It denotes the period during which dye molecules are subjected to the active catalyst surface while being exposed to light. Figure 9 presents the impact of contact time on removing dyes.

PP-Fe2O3-NPs achieve the highest DY3 removal rate, reaching nearly 89.21% in just 30 minutes and maintaining this level, as shown in Figure 10. MB also demonstrates notable efficiency, achieving 98.12% over time, while AO7 closely follows with a removal rate of 91.1%. Initially, RR5 shows a slower removal efficiency but eventually reaches approximately 86% over time.

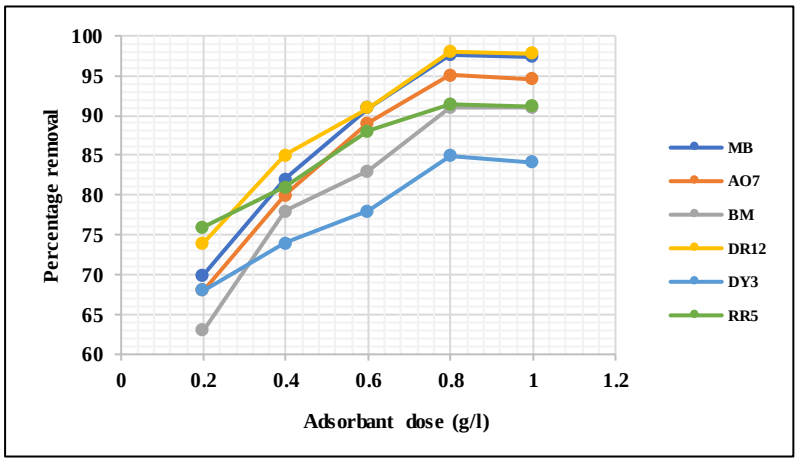

Fig. 7. Graphs showing the effect of the adsorbent dose on the percentage removal of dyes Pomegranate peel mediated Fe_2O_3NPs

Effect of contact time

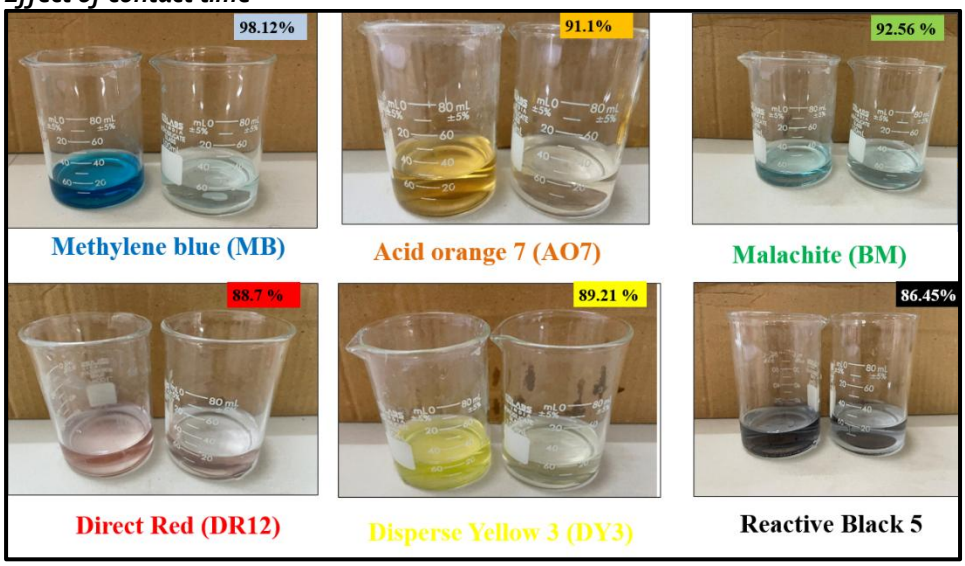

Fig. 9. Effect of contact time on decolouration of various dyes

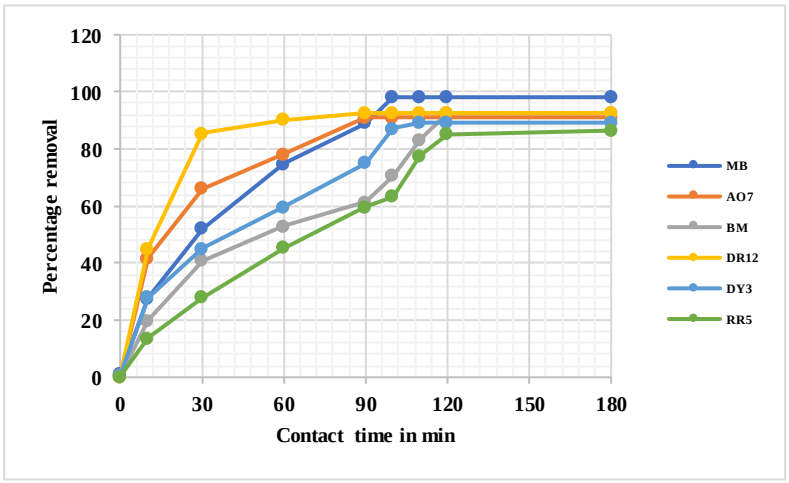

Fig. 8. Graphs showing the effect of contact time on the percentage removal of dyes Pomegranate peel mediated Fe_2O_3NPs

Conclusion

This research successfully developed an environmentally friendly, sustainable, and highly effective method for producing Iron Oxide Nanoparticles (Fe_2O_3) by utilizing the waste extract from *Punica granatum* (pomegranate) peel as the exclusive reducing and stabilizing agent. This green technique efficiently converts kitchen waste into a valuable catalytic material, perfectly aligning with the principles of waste valorisation and a circular economy. Comprehensive characterization (XRD, SEM, FTIR and EDS) confirmed that the synthesized Fe_2O_3NPs are crystalline having spherical morphology and with absorption peak between 270-320nm. FTIR analysis verified the

presence of surface-capping biomolecules from the pomegranate extract, which enhances the stability of the nanoparticles. The most notable discovery is the exceptional photocatalytic activity demonstrated by these biogenic Fe_2O_3NPs. Under solar light, the catalyst achieved rapid and nearly complete decolorization of Methylene Blue (98.12%) dye in a short period (100 minutes). The degradation process followed similar trends for other dyes as well, indicating high catalytic efficiency. In summary, this study not only introduces a green method for synthesizing advanced nanomaterials but also provides a powerful, cost-effective and magnetically recyclable photocatalyst for improved environmental remediation of organic dye pollutants. Future research will focus on optimizing the synthesis parameters to more precisely control particle size and exploring the applicability of these green Fe_2O_3NPs in degrading complex, real-world industrial effluents.

References

Abdulwahid FS, Haider AJ and Al-Musawi S (2022) Iron Oxide Nanoparticles (IONPs): Synthesis, Surface Functionalization, and Targeting Drug Delivery Strategies: Mini-Review. Nano 17(11):2230007. DOI-https://doi.org/10.1142/s1793292022300079

Badeenezhad A, Azhdarpoor A, Bahrami S and Yousefinejad S (2019) Removal of methylene blue dye from aqueous solutions by natural clinoptilolite and clinoptilolite modified by iron oxide nanoparticles. Molecular Simulation 45(7):564–571. DOI-https://doi.org/10.1080/08927022.2018.1564077

Bhuiyan MSH., Miah MY, Paul SC, et al. (2020) Green synthesis of iron oxide nanoparticle using Carica papaya leaf extract: application for photocatalytic degradation of Remazol yellow RR dye and antibacterial activity. Heliyon 6(8): e04603. https://doi.org/10.1016/j.heliyon.2020.e04603

Dadfar SM, Roemhild K, Drude NI, et al. (2019) Iron oxide nanoparticles: Diagnostic, therapeutic and theranostic applications. Advance Drug Delivery Review 138: 302-325, DOI: https://doi.org/10.1016/j.addr.2019.01.005

Gomathi AC, Xavier Rajarathinam SR, A. Mohammed Sadiq and S. Rajeshkumar (2020) Anticancer activity of silver nanoparticles synthesized using aqueous fruit shell extract of Tamarindus indica on MCF-7 human breast cancer cell line. Journal of Drug Delivery Science and Technology 55:101376. DOI- https://doi.org/10.1016/j.jddst.2019.101376

Habte L, Shiferaw N, Mulatu D, et al. (2019) Synthesis of nano-calcium oxide from waste eggshell by sol-gel method. Sustainability 11(11):3196. DOI- https://doi.org/10.3390/su11113196

Jahangirian H, Izadiyan Z, Kalantari K, et al. (2019) A review of small molecules and drug delivery applications using gold and iron nanoparticles. International Journal of Nanomedicine 14(9916):1633–1657. DOI-https://doi.org/10.2147/ijn.s184723

Krishnaswamy K, Vali H and Orsat V (2014) Value-adding to grape waste: Green synthesis of gold nanoparticles. Journal of Food Engineering 142:210–220. DOI- https://doi.org/10.1016/j.jfoodeng.2014.06.014

Majumder A, Ramrakhiani L, Mukherjee D, et al. (2019) Green synthesis of iron oxide nanoparticles for arsenic remediation in water and sludge utilization. Clean Technologies and Environmental Policy 21:795–813. DOI-https://doi.org/10.1007/s10098-019-016691

Nassar NN, Arar LA, Vitale G and Marei NN (2015) Adsorptive removal of dyes from synthetic and real textile wastewater using magnetic iron oxide nanoparticles: Thermodynamic and mechanistic insights. The Canadian Journal of Chemical Engineering 93(11):1965–1974. DOI- https://doi.org/10.1002/cjce.22315

Patel M, Siddiqi NJ, Sharma P, et al. (2019) Reproductive toxicity of pomegranate peel extracts synthesized gold nanoparticles: a multigeneration study in C. elegans. Journal of Nanomaterial 2019:1–7. DOI-https://doi.org/10.1155/2019/8767943

Patra JK, Kwon Y and Baek K-H (2016) Green biosynthesis of gold nanoparticles by onion peel extract: synthesis, characterization and biological activities. Advanced Powder Technology 27(5):2204–2213. DOI-https://doi.org/10.1016/j.apt.2016.08.005

Phang Y-K, Aminuzzaman M, Akhtaruzzaman M, et al. (2021) Green Synthesis and Characterization of CuO Nanoparticles Derived from Papaya Peel Extract for the Photocatalytic Degradation of Palm Oil Mill Effluent (POME) Sustainability, 13(2):796. DOI- https://doi.org/10.3390/su13020796

Rathnasamy R, Thangasamy P, Thangamuthu R, Sampath S and Alagan V (2017) Green synthesis of ZnO nanoparticles using Carica papaya leaf extracts for photocatalytic and photovoltaic applications. Journal of Materials Science: Materials in Electronics 28(14):10374–10381. DOI- https://doi.org/10.1007/s10854-017-6807-8

Siciliano G, Monteduro AG, Depalo N, et al. (2022) Polydopamine-Coated Magnetic Iron Oxide Nanoparticles: From Design to Applications. Nanomaterials 12(7):1145. DOI- https://doi.org/10.3390/nano12071145

Siwal SS, Zhang Q, Devi N, et al. (2021) Recovery processes of sustainable energy using different biomass and wastes. Renewable and Sustainable Energy Reviews 150:111483. DOI: https://doi.org/10.1016/j.rser.2021.111483

Skiba MI and Vorobyova VI (2019) Synthesis of silver nanoparticles using orange peel extract prepared by plasmochemical extraction method and degradation of methylene blue under solar irradiation. Advances in Materials Science Engineering 2019:1–8. DOI- https://doi.org/10.1155/2019/8306015

Thacker H, Ram V and Dave P (2019) Plant mediated synthesis of Iron nanoparticles and their Applications: A Review. Progress in Chemical and Biochemical Research 2(3): 84–91.DOI-https://doi.org/10.33945/sami/pcbr.2019.183239.1033

Venkateswarlu S, Subba Rao Y, Balaji T, et al. (2013) Biogenic synthesis of Fe_3O_4 magnetic nanoparticles using plantain peel extract. Materials Letters 100:241-244. DOI- https://doi.org/10.1016/j.matlet.2013.03.018

Vishwasrao C, Momin B and Ananthanarayan L (2019) Green synthesis of silver nanoparticles using sapota fruit waste and evaluation of their antimicrobial activity. Waste and Biomass Valorization 10(8):2353–2363. DOI-https://doi.org/10.1007/s12649-018-0230-0

Wang K, Xu X-G, Ma Y-L, et al. (2020) Fe_3O_4@Angelica sinensis polysaccharide nanoparticles as an ultralow-toxicity contrast agent for magnetic resonance imaging. Rare Metals, 40(9):2486–2493.DOI-https://doi.org/10.1007/s12598-020-01620-0

Author Contributions
NG and AV conceived the concept, wrote and approved the manuscript.

Acknowledgements
Not applicable.

Funding
Not applicable.

Availability of data and materials
Not applicable.

Competing interest
The authors declare no competing interests.

Ethics approval
Not applicable.

Citation: Gaur N and Verma A (2026) Valorizing Kitchen Waste into Potent Nano-Remediators: A Green Synthesis of Iron Oxide Nanoparticles using *Punica granatum* for Efficient Industrial Dye Decolouration. Environmental Science Archives 5(1): 58-65.